

Efficient Hepatitis C Virus Particle Formation Requires Diacylglycerol Acyltransferase 1 (DGAT1)

Eva Herker, Charles Harris, Céline Hernandez, Arnaud Carpentier, Katrin Kaehlcke,
Arielle R. Rosenberg, Robert V. Farese Jr, and Melanie Ott

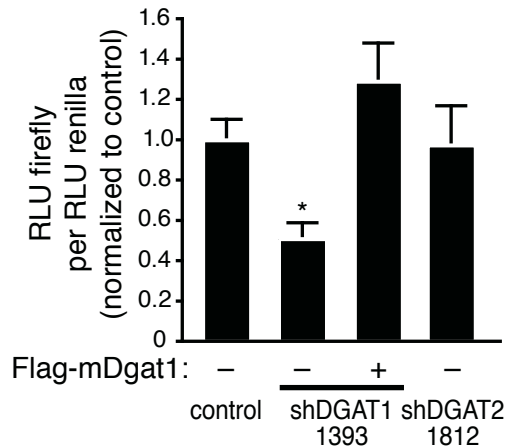
Supplementary Information

Contents:

Supplementary Figures 1–7

Supplementary Methods

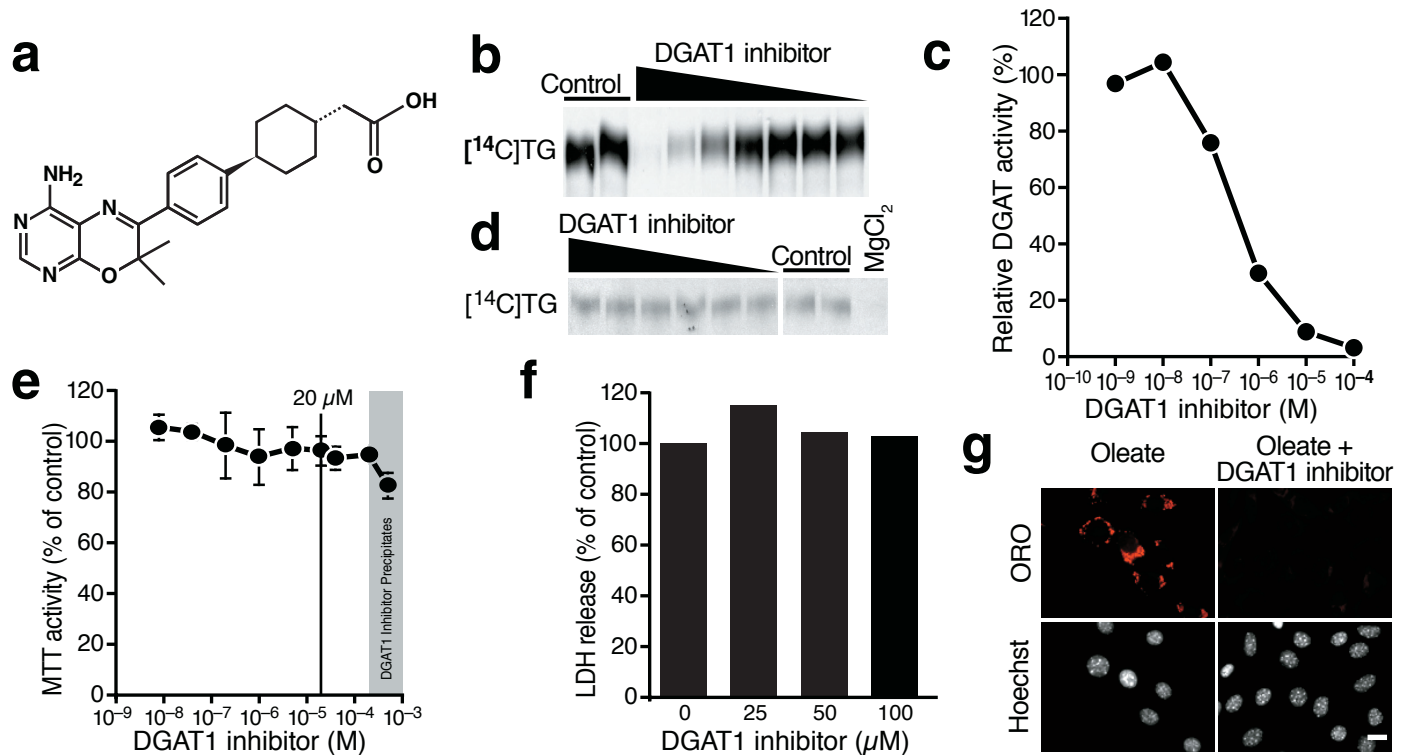
Supplementary Figure 1



Supplementary Figure S1: Rescue of HCV particle production by overexpression of shRNA-resistant DGAT1

Huh7.5 cells transduced with shRNA 1393 directed against DGAT1 were cotransfected with Luciferase-Jc1 RNA and an expression construct for murine Dgat1 carrying a 2-nucleotide mismatch to 1393 (shRNA 1393: GGAACATCCCTGTGCACAA, *mDgat1*: GGAATATCCCCGTGCACAA). A construct expressing renilla luciferase was also cotransfected to normalize transfection efficiencies at 4 h post transfection. Naïve Huh7.5 cells were infected with cell supernatants of transfected cells and lysed 48 h post infection for luciferase assays (expressed as RLU firefly per RLU renilla, normalized to control cells; mean \pm s.e.m., $n = 8$, $*p < 0.05$). Coexpression of Dgat1 reversed the decrease in viral particle production caused by DGAT1 shRNA 1393 while knockdown of DGAT2 had no effect.

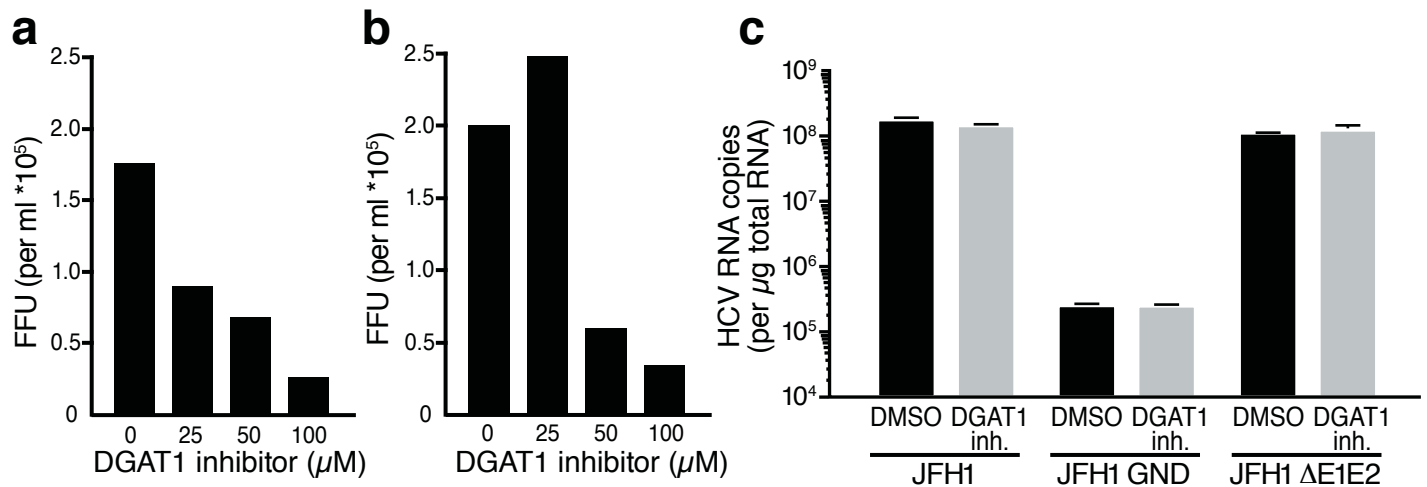
Supplementary Figure 2



Supplementary Figure S2: Structure and validation of the DGAT1 inhibitor

(a) Structure of 2-((1s,4s)-4-(4-(4-amino-7,7-dimethyl-7H-pyrimido[4,5-b][1,4]oxazin-6-yl)phenyl)cyclohexyl)acetic acid, a pharmaceutical DGAT1 inhibitor. (b) *In vitro* DGAT activity assay of cell lysates of Sf9 cells infected with a DGAT1-expressing baculovirus and pretreated with decreasing amounts of the DGAT1 inhibitor (100 μ M to 1 nM). Extracted lipids were loaded on a thin layer chromatography plate and analyzed by autoradiography. (c) Quantification of b). For the determination of the IC_{50} of the DGAT1 inhibitor, DGAT1 activity in the absence of the DGAT1 inhibitor was set at 100%. The IC_{50} of the DGAT1 inhibitor in this *in vitro* assay is \sim 300 nM. (d) *In vitro* DGAT activity assay using liver homogenates of DGAT1^{-/-} mice pretreated with decreasing amounts of the DGAT1 inhibitor ranging from 100 μ M to 1 nM. MgCl₂ (100 mM) was added as a positive control to inhibit DGAT2 activity¹. Extracted lipids were loaded on a thin layer chromatography plate and analyzed by autoradiography. No effect of the DGAT1 inhibitor on DGAT2 activity was observed. (e) Cytotoxicity (MTT) assay of Huh7.5 cells treated with increasing amounts of the DGAT1 inhibitor for 48 h. Shown are values as percent of DMSO control-treated cells (mean of eight replicates \pm s.d.). No cytotoxicity of the DGAT1 inhibitor was observed below concentrations of 200 μ M. At higher concentrations, we observed precipitation of the inhibitor and slight cytotoxic effects. (f) Cytotoxicity (LDH release) assay of primary human hepatocytes treated with the DGAT1 inhibitor. Shown are values as percent of DMSO control-treated cells. (g) Epifluorescence microscopy of NIH/3T3 cells incubated with 20 μ M DGAT1 inhibitor or DMSO for 24 h, loaded with 300 μ M BSA-bound oleate for 16 h, fixed and incubated with oil-red-O (ORO) to visualize lipid droplets (scale bar = 10 μ m). DGAT1 inhibition completely suppressed lipid droplet formation in cultured NIH/3T3 cells, demonstrating that the inhibitor *in vivo* suppresses DGAT1 activity in cells and that DGAT1 is the prominent DGAT enzyme NIH/3T3 cells.

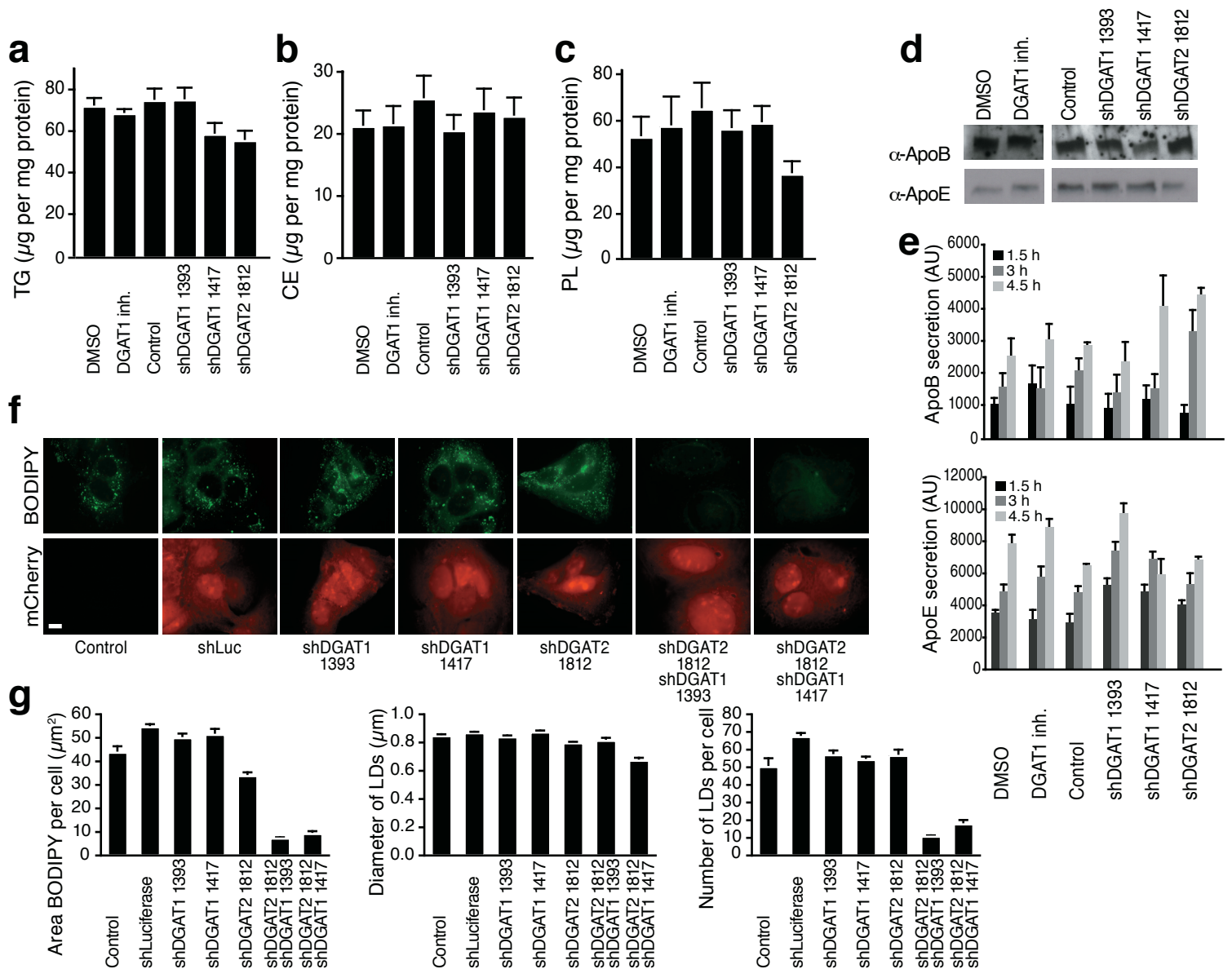
Supplementary Figure 3



Supplementary Figure S3: Antiviral effect of DGAT1 inhibition in hepatoma cells and primary human hepatocytes

(a–b) Huh7.5.1 cells (a) and freshly isolated primary human hepatocytes (b) were infected with HCV-Jc1 and treated with increasing amounts of the DGAT1 inhibitor or DMSO control for 3 days. Infectivity titers in culture supernatants were determined by focus-formation assays, as previously described². Shown are focus-forming units (FFU) per ml culture supernatant. (c) Two previously characterized mutants in the HCV-JFH1 background³ were used to demonstrate that newly generated viral RNA was measured in cells: JFH1 GND expresses inactive viral RNA-dependent RNA polymerase (no RNA replication), JFH1 ΔE1E2 lacks envelope protein expression (no viral particle production, mimics RNA ‘replicons’). Huh7.5 cells were electroporated with *in vitro* transcribed JFH1, JFH1 GND and JFH1 ΔE1E2 RNA (day 0) and treated with DMSO or 20 μM DGAT1 inhibitor (day 1). Intracellular HCV RNA was quantified by real-time RT-PCR (mean \pm s.d., $n = 3$) normalized to 18S rRNA. A three-log difference in intracellular HCV RNA levels was observed between cells transfected with actively replicating wildtype JFH1 virus versus cells transfected with the GND mutant indicating that newly generated, and not transfected input HCV RNAs are measured. No effect of DGAT inhibition was observed on intracellular HCV RNA levels of JFH1 or JFH1 ΔE1E2 , confirming that DGAT1 inhibition has no effect on HCV RNA replication.

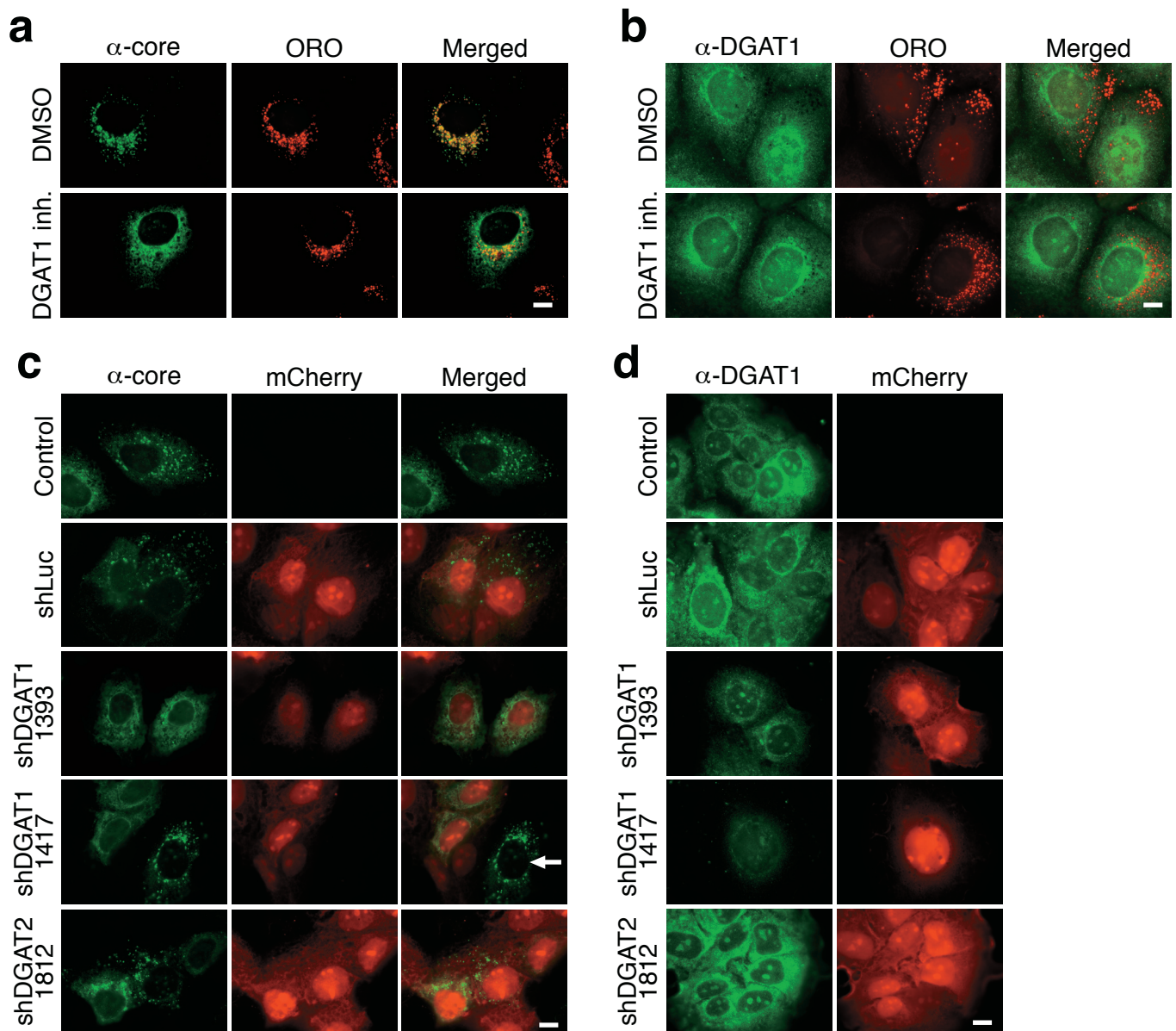
Supplementary Figure 4



Supplementary Figure S4: Effect of DGAT1 inhibition or DGAT1/DGAT2 knockdown on triglyceride, cholesterol ester, and phospholipid content and the secretion of lipoproteins

Huh7.5 cells were treated with 20 μM of the DGAT1 inhibitor or DMSO control for 48 h or transduced with lentiviral expression constructs targeting DGAT1 or DGAT2. Triglycerides (a) were quantified by thin-layer chromatography, cholesterol ester (b) and phospholipids (c) were quantified using commercial assays (mean \pm s.e.m., (a): $n = 3$, (b and c): $n = 6$). (d) Lipoprotein secretion was assessed by western blotting of culture supernatant with α -ApoB100 and α -ApoE antibodies as described^{4,5}. To exclude cross-reaction with serum proteins, cells were washed three times in serum-free media (Opti-MEM) and cultured for 3 h in serum-free media. (e) Quantification of time-dependent ApoB100 and ApoE secretion by densitometric analysis with Image J software of western blots (mean \pm s.e.m., $n = 3$). No change in triglyceride, cholesterol ester, and phospholipid content or lipoprotein secretion was detected after inhibition of DGAT1 or knockdown of DGAT1 or DGAT2, indicating that in hepatoma cells DGAT1 and DGAT2 have redundant functions. (f) BODIPY staining to visualize lipid droplet content in cells transduced with DGAT1 and/or DGAT2 shRNA lentiviral vectors (scale bar = 10 μm). (g) Quantification of f). Lipid droplet area: mean of > 50 cells \pm s.e.m.; lipid droplet diameter: mean of > 50 lipid droplets \pm s.e.m.; lipid droplet number: mean of > 50 cells \pm s.e.m.. While single knockdown of either DGAT enzyme did not decrease the amount or number of lipid droplets in hepatoma cells, double knockdown of DGAT1 and DGAT2 significantly reduced the area of lipid droplets in cells and the number of lipid droplets. No effect on the average lipid droplet size was observed.

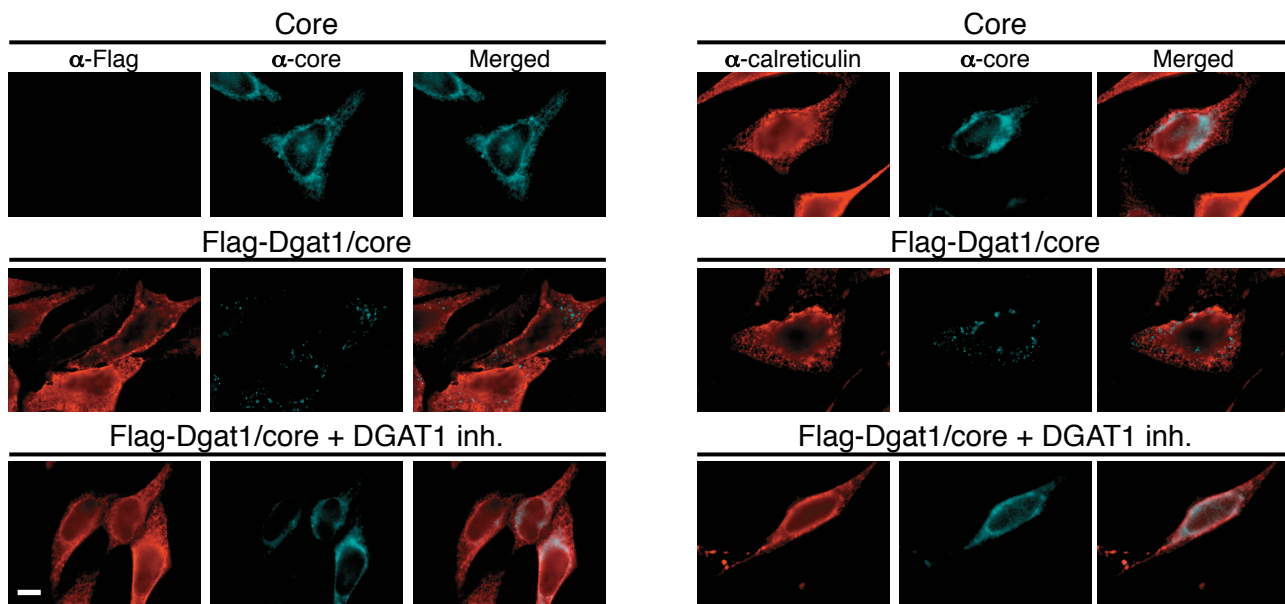
Supplementary Figure 5



Supplementary Figure S5: DGAT1 inhibition or DGAT1 knockdown causes retention of the core protein at the ER

(a–b) Huh7 cells were transfected with core expressing plasmids or left untransfected and treated with 20 μ M of the DGAT1 inhibitor or DMSO control. Cells were fixed and stained with α -core (a) or α -DGAT1 (b) antibodies and oil-red-O (ORO) before epifluorescence microscopy. (a) While in control cells core readily localizes to lipid droplets, in DGAT1 inhibitor-treated cells, the majority of core remains at reticular structures, which do not colocalize with lipid droplets. (b) DGAT1 inhibition does not change the subcellular localization of DGAT1. (c–d) Huh7.5 cells transduced with lentiviral shRNA vectors targeting DGAT1 or DGAT2 were transfected with HCV core expression plasmids or left untransfected. Cells were fixed and stained with α -core (c) or α -DGAT1 (d) antibodies and analyzed by epifluorescence microscopy. (c) In control and DGAT2 knockdown cells, core localized to punctuate cytosolic structures (lipid droplets), while in DGAT1 knockdown cells, a reticular pattern (ER) was observed. Of note, in shDGAT1 1417-transduced cells a neighboring mCherry-negative cell (not harboring the shRNA) is depicted in which core is localized at lipid droplets (arrow). (d) DGAT2 knockdown has no effect on DGAT1 subcellular localization. In DGAT1 knockdown cells, DGAT1 staining is decreased, confirming the knockdown observed in western blotting and real-time RT-PCR (scale bars = 10 μ m).

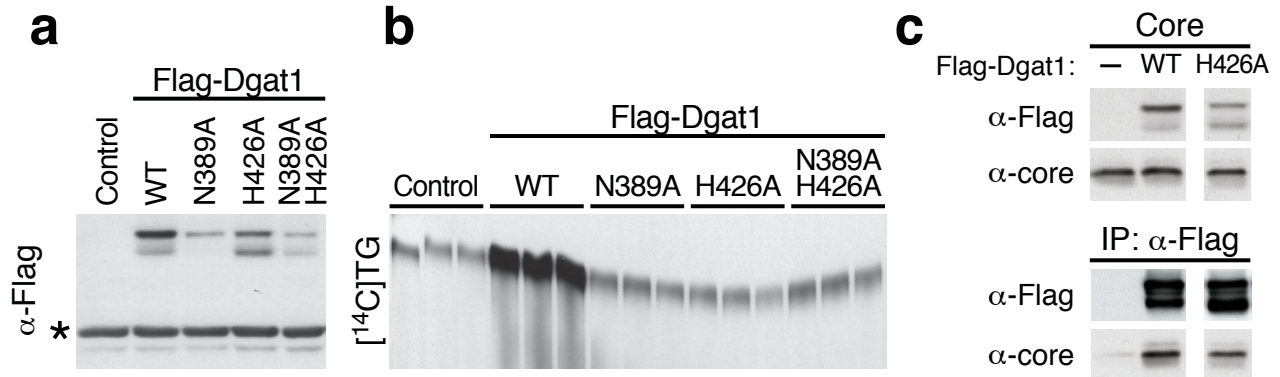
Supplementary Figure 6



Supplementary Figure S6: Overexpression of active Dgat1 translocates core to lipid droplets

HeLa cells were cotransfected with expression constructs for core and/or Flag-Dgat1. Cells expressing core and Flag-Dgat1 were subsequently treated with 20 μ M DGAT1 inhibitor. After fixation, cells were immunostained with antibodies directed against Flag and core or calreticulin and core. In the absence of Flag-Dgat1, core localizes to reticular structures (ER), while coexpression of Flag-Dgat1 readily translocates core to lipid droplets. In cells treated with the DGAT1 inhibitor, core is retained at the ER despite the presence of Flag-Dgat1 (scale bar = 10 μ m).

Supplementary Figure 7



Supplementary Figure S7: The catalytic activity of Dgat1 is not required for its interaction with core

We introduced two point mutations (N389A and H426A) in the predicted catalytic domain of Flag-Dgat1 based on alignments with structurally related enzymes. **(a)** Western blotting with α -Flag antibodies of 293T cells after transfection. * marks a nonspecific band that serves as loading control. Flag-Dgat1 (N389A) and the double mutant are not well expressed. **(b)** *In vitro* DGAT activity assay. Lysates of transfected cells were incubated with diacylglycerol and radioactive oleoyl-coenzyme A. Extracted lipids were loaded on a thin layer chromatography plate and analyzed by autoradiography. The assay is shown in triplicates. Bands in control lanes represent endogenous DGAT activity, but no activity of the mutant Flag-Dgat1 proteins was observed. **(c)** Coimmunoprecipitation of the HCV core protein and Flag-Dgat1 or Flag-Dgat1 (H426A) in 293T cells. Core efficiently coimmunoprecipitated with catalytically inactive Dgat1 (H426A), supporting that core binding to Dgat1 does not require the catalytic activity of Dgat1.

Supplementary Methods

Plasmids

To generate the bicistronic lentiviral core expression construct, the 191–amino acid core coding sequence (genotype 1b, NC1) was cloned into a modified version of the lentiviral pHR⁷ vector⁶ containing a minimal nonreplicative HIV-1 genome, a heterologous promoter (EF-1 α) driving core expression, followed by the IRES of ECMV driving expression of eGFP. The SPMT core mutant was constructed by site-directed mutagenesis (Stratagene) as described⁷. Core constructs without the IRES-eGFP marker were cloned into pEBB expression vector⁸. Flag-tagged murine Dgat1 and Dgat2 expression constructs were as described⁹. Point-mutants of Dgat1 were constructed by site-directed mutagenesis (Stratagene) of conserved residues within the family of membrane-bound O-acyltransferases¹⁰ that are required for catalytic activity (N389A and H426A). The baculovirus expressing Dgat1 was as described¹¹. Jc1, Luciferase-Jc1, and Luciferase-JFH1 have been described¹². eGFP-Jc1 and eGFP-JFH1 reporter viruses were generated by cloning eGFP in place of luciferase into the bicistronic reporter viruses¹². Small hairpin RNAs targeting DGAT1 (1393: GGAACATCCCTGTGCACAA, 1417: GCATCAGACACTTCTACAA), and DGAT2 (1812: GCGAAAGCCACTTCTCATA), and luciferase (CTTACGCTGAGTACTTCGA) were cloned into a modified version of the pSicoR lentiviral vector that encodes a mCherry reporter driven by an EF-1 α promoter (pSicoRMS)^{13,14}.

Cell lines and culture conditions

Huh7 and HEK293T cells were obtained from the American Type Culture Collection, Huh7.5 cells from Charles M. Rice, Huh7 Lunet cells from Ralf Bartenschlager, and

Huh7.5.1 from Francis V. Chisari. All cells were grown under standard cell culture conditions and transfected with FuGENE6 (Roche), according to the manufacturer's protocol. Calcium phosphate-mediated transfection of HEK293T cells was used for the production of lentiviral particles. Huh7.5 cells were used for HCV infection experiments because of their high level CD81 expression¹⁵, while Huh7 Lunet were used for the microscopy studies due to their superior properties for immunofluorescence microscopy¹⁶. Viral RNA replication and infectious virus release are similar in both cell lines¹⁵.

Antibodies and reagents

The following antibodies were obtained commercially: α -core (clone C7-50; Affinity BioReagents), α -NS3 (#1849, ViroStat), α -NS5A (#1827, ViroStat), α -dsRNA (J2, Scicons), α -DGAT1 (H-255, Santa Cruz), α -Tubulin (T6074, Sigma), α -ADRP (H-80, Santa Cruz), α -Calreticulin (SPA-600, Stressgen), α -KDEL/BiP (SPA-827, Stressgen), α -ApoB100 (ab31992, Abcam), α -ApoE (178479, Calbiochem), α -Flag M2 (Sigma), α -Flag (F7425, Sigma), α -mouse Alexa 647 (Invitrogen), α -mouse Alexa 594 (Invitrogen), α -rabbit Alexa 488 (Invitrogen), α -rabbit Cy3 (Jackson ImmunoResearch Laboratories), and α -mouse Cy5 (Jackson ImmunoResearch Laboratories). The DGAT1 inhibitor (2-((1s,4s)-4-(4-(4-amino-7,7-dimethyl-7H-pyrimido[4,5-b][1,4]oxazin-6-yl)phenyl)cyclohexyl)acetic acid) was synthesized by Syngene International, according to public disclosures¹⁷. BSA-bound oleate was purchased from Sigma and CellTiter 96 Non-Radioactive Cell Proliferation Assay and CytoTox 96 Non-Radioactive Cytotoxicity Assay from Promega. Enzymes for molecular cloning were purchased from New England

Biolabs, cell culture reagents from Invitrogen, and fine chemicals, if not noted otherwise, from Sigma.

Immunofluorescence and oil-red-O staining

Cells grown on coverslips were fixed in 3.7% paraformaldehyde for 30–60 min at room temperature, washed with phosphate-buffered saline (PBS), and permeabilized in 0.1% Triton X-100 for 5 min. After incubation in blocking solution (5% BSA, 1% fish skin gelatin, 50 mM Tris in PBS) cells were incubated with primary antibodies in blocking solution for 45 min at room temperature, washed and incubated with secondary antibodies for 45 min at room temperature. For oil-red-O (ORO) staining coverslips were incubated for 5 min in 60% isopropanol and stained with ORO staining solution (stock: 0.5 g ORO (Sigma) in 100 ml of isopropanol; the stock was diluted 6:4 (stock:water) and filtered before use) and differentiated in 60% isopropanol for 1 sec and embedded in Mowiol (Calbiochem) mounting medium¹⁸. For BODIPY staining, fixed cells were stained for 20 min with 1 $\mu\text{g ml}^{-1}$ BODIPY 493/503 in PBS. For the quantification of lipid droplets per cell, we stained the nuclei with Hoechst (Sigma). For loading of cells with oleate, cells were incubated in the presence of 300 μM BSA-bound oleate (Sigma) for the indicated times.

Epifluorescence microscopy and quantification of images

Cells were analyzed with an Axio observer Z1 microscope (Zeiss) equipped with EC Plan Neofluar 20X/0.5 PHM27, EC Plan Neofluar 40X/0.75 PH, and Plan Apo 63X/1.4 Oil DIC M27 objectives, filter sets 38HE, 43HE, 45, and 50, Optovar 1.25 and 1.6X magnification, and an Axiocam MRM REV 3. For quantification of lipid droplets we used the automatic measurement program of the Zeiss axiovision software.

Lentivirus production and transduction

Lentiviral particles were produced as described⁶. Briefly, 293T cells were cotransfected with the transfer plasmid encoding core-IRES-eGFP or the pSicoRMS shRNA constructs, an HIV-based packaging construct (pCMVΔR8.91), and a construct expressing the glycoprotein of vesicular stomatitis virus (VSV-G) (pMD.G). Culture supernatant containing pseudotyped lentiviral particles was concentrated using ultracentrifugation for 16 h at 20,000 rpm in a SW28 rotor. Infectious titres were determined by transducing cells with serial dilutions of the viral stocks and FACS analysis 2 days post-transduction. Transductions were carried out in the presence of 4 μg ml⁻¹ polybrene (Sigma) for 4 h at 37 °C.

Immunoprecipitation, lipid droplet isolation and western blotting

For immunoprecipitation experiments, cells were lysed in lysis-buffer (150 mM NaCl, 1% NP-40, 1 mM EDTA, 50 mM Tris HCl, pH 7.4 and protease inhibitor cocktail (Sigma)) for 30 min and passed 10 times through a G23 needle. Clarified lysates were immunoprecipitated with α-Flag M2 agarose (Sigma) or DGAT1 antibody and protein A agarose (Invitrogen), washed 5 times in lysis buffer and resuspended in Laemmli buffer for SDS-PAGE.

Lipid droplets were isolated as described¹⁹. Briefly, cells were scraped in PBS, lysed in hypotonic buffer (50 mM HEPES, 1 mM EDTA and 2 mM MgCl₂, pH 7.4) supplemented with protease inhibitors with 30 strokes in a tight-fitting Dounce homogenizer. After spinning 5 min at 1500 rpm, post-nuclear fractions were mixed with equal volumes of 1.05 M sucrose in isotonic buffer (50 mM HEPES, 100 mM KCl, 2 mM MgCl₂) and placed at the bottom of SW55 Ti (Beckman) centrifuge tubes, overlaid with

isotonic buffer containing 1 mM PMSF and centrifuged for 2 h at 100,000 g. Proteins from the floating lipid droplet fraction were precipitated with 15% trichloroacetic acid and 30% acetone, washed once with acetone and resuspended in urea loading dye (200 mM Tris/HCl, pH 6.8, 8 M urea, 5% SDS, 1 mM EDTA, 0.1% bromophenol blue, 15 mM DTT).

For western blot analysis, cells were lysed in RIPA buffer (1% NP-40, 0.5% sodium deoxycholate, 0.1% SDS in PBS supplemented with protease inhibitor cocktail (Sigma)) for 30 min, followed by SDS-PAGE. For chemiluminescent detection, we used ECL and ECL Hyperfilm (Amersham).

***In vitro* transcription of HCV RNA and transfection**

Plasmids encoding HCV reporter viruses were linearized with XbaI and purified by phenol-chloroform extraction. *In vitro* transcription was carried out using the MegaScript T7 kit (Ambion), according to the manufacturers protocol. RNA was further purified using the RNeasy Mini Kit (Qiagen). For RNA transfection, Huh7.5 or Huh7 Lunet cells were trypsinized, washed once in Opti-MEM (Invitrogen), and resuspended in Cytomix buffer (120 mM KCl, 5 mM MgCl₂, 0.15 mM CaCl₂, 2 mM EGTA, 1.9 mM ATP, 4.7 mM GSH, 25 mM HEPES, 10 mM potassium phosphate buffer, pH 7.6) at 10⁷ cells ml⁻¹. 400 µl of the cell suspension were mixed with 10 µg HCV RNA and pulsed at 260 V and 950 µF with the Gene Pulser II (Biorad).

HCV virus concentration, infection and FACS and Luciferase analysis

Culture supernatant of Huh7.5 cells transfected with HCV RNA was harvested, filtered and concentrated by ultrafiltration using Amicon Ultra-15 100 kDa filtration devices (Millipore) or left unconcentrated. For infection experiments, naïve Huh7.5 were

plated on 24-well plates, infected with virus for 3 h at 37°C. Cells infected with the eGFP reporter viruses were harvested by trypsinization, fixed in 1% paraformaldehyde for 1 h, and analyzed by flow cytometry using FACS Calibur or LSR-II (BD Biosciences) and FlowJo software (TreeStar). Cells infected with the luciferase reporter viruses were lysed in 1x lysis buffer (Promega). Luciferase activity was measured using Luciferase or Dual-Luciferase Assay Systems (Promega) on a MonoLight 2010 Luminometer (Pegasus Scientific Inc.).

HCV infection of primary human hepatocytes and titration of infectivity

Normal-appearing liver tissue was obtained from HCV-seronegative adult patients undergoing partial hepatectomy for the therapy of metastases. Experimental procedures were carried out in accord with French laws and regulations. Dissociation of liver cells was performed by a two-step perfusion method, as described²⁰. Hepatocytes were resuspended in complete medium consisting of Leibovitz's L-15 medium (Invitrogen) supplemented with 26 mM NaHCO₃, 100 IU I⁻¹ insulin (Novo Nordisk) and 10% heat-inactivated fetal calf serum (Biowest), and seeded onto 6-well plates pre-coated with calf skin type I collagen (Sigma) at a density of 1.2 x 10⁵ viable cells cm⁻². The medium was replaced 16 h later with fresh complete medium, supplemented with 1 μM hydrocortisone hemisuccinate (SERB), and the cultures were maintained at 37°C in a humidified 5% CO₂ atmosphere. Three days later, the monolayers were inoculated at a multiplicity of infection of 0.1 focus-forming units (FFU) per cell with HCV-Jc1 grown in Huh7.5.1 cells²¹ and concentrated as described above. After overnight incubation at 37°C, the inoculum was removed, and monolayers were washed three times with PBS. The cultures were then continued for 3 days in complete medium containing 0.5% DMSO as carrier

control, or else increasing concentrations of DGAT1 inhibitor. Infectivity titers in culture supernatants were determined by focus-formation assay, as described².

RNA isolation and real-time RT-PCR

Total cellular RNA was isolated using RNA Stat reagent (TelTest) according to the manufacturer's protocol and treated with the TURBO DNA-free DNase (Ambion). Viral RNA from the culture supernatant was isolated with the MagMAX Viral RNA Isolation Kit (Ambion). RNA levels were adjusted to carrier RNA input that was added in excess prior to RNA isolation. cDNA was synthesized using Superscript III reverse transcriptase (Invitrogen) with random hexamer primers, followed by RNase H (New England Biolabs) digestion. For real-time PCR, we used HCV-specific primers and a Taqman probe (Applied Biosystems) as described³ (sense: 5'-CGGGAGAGCCATAGTGG-3', antisense: 5'-AGTACCACAAGGCCTTTCG-3', probe: 5'-CTGCGGAACCGGTGAGTACAC-3'), as well as pre-designed 18S rRNA, DGAT1, and DGAT2 Taqman assays (Applied Biosystems). Real-time PCR was performed using QuantiTect Probe PCR Kit (Qiagen) on a 7900HT Fast Real-time RT-PCR System (Applied Biosystems).

DGAT activity assay and measurement of triglycerides, cholesterolesters, and phospholipids

DGAT assays were performed as described¹¹. Briefly, cells were lysed in DGAT assay buffer (250 mM sucrose, 50 mM Tris HCl, pH 7.4) and passed through a G30 needle. 50 µg protein was used in a reaction containing 200 µM diacylglycerol dissolved in acetone, 25 µM oleoyl-CoA (0.9 µCi µmol⁻¹, American Radiolabeled Chemicals), 10 mM MgCl₂, and 0.625 mg ml⁻¹ BSA. After incubation for 5 min at 37°C, the reaction

was terminated with chloroform:methanol (2:1 v/v). After mixing with water, the organic fraction was extracted, dried, loaded onto thin layer chromatography plates, and quantified using a Bioscan AR-2000 instrument.

For the determination of the IC₅₀ of the DGAT1 inhibitor, Dgat1 was overexpressed in Sf9 insect cells with a baculoviral construct¹¹, and reactions were performed as described above. Activity in the absence of inhibitor was considered as 100%.

Triglycerides were isolated by hexane:isopropanol (3:2 v/v) extraction, and after evaporation of the solvent under nitrogen stream, samples were loaded onto thin layer chromatography plates. Plates were dipped in 10% cupric sulfate in 8.4% phosphoric acid, heated at 160°C for 10 min, and triglycerides were quantified against a standard by densitometry with ImageJ. Cholesterol ester and phospholipids were quantified using commercial assays (Wako).

Statistical analysis

Statistical analysis was performed using unpaired two-tailed student's t-test.

Supplementary References

1. Cases, S., *et al.* Cloning of DGAT2, a second mammalian diacylglycerol acyltransferase, and related family members. *J. Biol. Chem.* **276**, 38870-38876 (2001).
2. Pene, V., Hernandez, C., Vauloup-Fellous, C., Garaud-Aunis, J. & Rosenberg, A.R. Sequential processing of hepatitis C virus core protein by host cell signal peptidase and signal peptide peptidase: a reassessment. *J. Viral Hepat.* **16**, 705-715 (2009).
3. Wakita, T., *et al.* Production of infectious hepatitis C virus in tissue culture from a cloned viral genome. *Nat. Med.* **11**, 791-796 (2005).
4. Chang, K.S., Jiang, J., Cai, Z. & Luo, G. Human apolipoprotein e is required for infectivity and production of hepatitis C virus in cell culture. *J. Virol.* **81**, 13783-13793 (2007).
5. Huang, H., *et al.* Hepatitis C virus production by human hepatocytes dependent on assembly and secretion of very low-density lipoproteins. *Proc. Natl. Acad. Sci. U.S.A.* **104**, 5848-5853 (2007).
6. Naldini, L., *et al.* In vivo gene delivery and stable transduction of nondividing cells by a lentiviral vector. *Science* **272**, 263-267. (1996).
7. McLauchlan, J., Lemberg, M.K., Hope, G. & Martoglio, B. Intramembrane proteolysis promotes trafficking of hepatitis C virus core protein to lipid droplets. *EMBO J.* **21**, 3980-3988 (2002).

8. Tanaka, M., Gupta, R. & Mayer, B.J. Differential inhibition of signaling pathways by dominant-negative SH2/SH3 adapter proteins. *Mol. Cell. Biol.* **15**, 6829-6837 (1995).
9. Stone, S.J., et al. The endoplasmic reticulum enzyme DGAT2 is found in mitochondria-associated membranes and has a mitochondrial targeting signal that promotes its association with mitochondria. *J. Biol. Chem.* **284**, 5352-5361 (2009).
10. Hofmann, K. A superfamily of membrane-bound O-acyltransferases with implications for wnt signaling. *Trends Biochem. Sci.* **25**, 111-112 (2000).
11. Cases, S., et al. Identification of a gene encoding an acyl CoA:diacylglycerol acyltransferase, a key enzyme in triacylglycerol synthesis. *Proc. Natl. Acad. Sci. U.S.A.* **95**, 13018-13023 (1998).
12. Pietschmann, T., et al. Construction and characterization of infectious intragenotypic and intergenotypic hepatitis C virus chimeras. *Proc. Natl. Acad. Sci. U.S.A.* **103**, 7408-7413 (2006).
13. Ventura, A., et al. Cre-lox-regulated conditional RNA interference from transgenes. *Proc. Natl. Acad. Sci. U.S.A.* **101**, 10380-10385 (2004).
14. Grskovic, M., Chaivorapol, C., Gaspar-Maia, A., Li, H. & Ramalho-Santos, M. Systematic identification of cis-regulatory sequences active in mouse and human embryonic stem cells. *PLoS Genet.* **3**, e145 (2007).
15. Koutsoudakis, G., Herrmann, E., Kallis, S., Bartenschlager, R. & Pietschmann, T. The level of CD81 cell surface expression is a key determinant for productive entry of hepatitis C virus into host cells. *J. Virol.* **81**, 588-598 (2007).

16. Shavinskaya, A., Boulant, S., Penin, F., McLauchlan, J. & Bartenschlager, R. The lipid droplet binding domain of hepatitis C virus core protein is a major determinant for efficient virus assembly. *J. Biol. Chem.* **282**, 37158-37169 (2007).
17. Amgen and JT Pharma. ANORECTIC COMPOUNDS. *World Intellectual Property Organization* **WO/2005/072740**.
18. Longin, A., Souchier, C., Ffrench, M. & Bryon, P.A. Comparison of anti-fading agents used in fluorescence microscopy: image analysis and laser confocal microscopy study. *J. Histochem. Cytochem.* **41**, 1833-1840 (1993).
19. Miyanari, Y., *et al.* The lipid droplet is an important organelle for hepatitis C virus production. *Nat. Cell Biol.* **9**, 1089-1097 (2007).
20. Podevin, P., *et al.* Production of infectious hepatitis C virus in primary cultures of human adult hepatocytes. *Gastroenterology*, doi:10.1053/j.gastro.2010.06.058 (2010).
21. Zhong, J., *et al.* Robust hepatitis C virus infection in vitro. *Proc. Natl. Acad. Sci. U.S.A.* **102**, 9294-9299 (2005).